Digital Signal Processing 111 (2021) 102976

Contents lists available at ScienceDirect

Digital Signal Processing

www.elsevier.com/locate/dsp

Narrowband feedback active noise control systems with secondary path modeling using gain-controlled additive random noise

Muhammad Tahir Akhtar

Department of Electrical and Computer Engineering, School of Engineering & Digital Sciences, Nazarbayev University, Nur-Sultan, Kazakhstan

ARTICLE INFO

Article history:
Available online 18 January 2021

Keywords:
Active noise control
FxLMS algorithm
Feedback-type ANC
Secondary path modeling
Modeling signal

ABSTRACT

This paper investigates estimation of the secondary path (SP) during the online operation of the filtered-*x* least mean square (FxLMS) algorithm-based feedback active noise control (FBANC) systems. The proposed method develops upon a previous work where two adaptive filters were used, one for active noise control (ANC) and the other for secondary path modeling (SPM). The proposed method essentially comprises a similar structure as that of the previous method. The objectives here are to suggest modifications to improve upon the slow convergence of SPM filter and the noise reduction (NR) performance in the previous method. The key idea is to employ a gain-controlled modeling signal (generated from the additive random noise signal) mixed with the cancellation signal. The gain-factor for the modeling signal is adjusted such that a large-level modeling signal is used during the transient state of the ANC system. This improves the converge of the SPM filter. As the ANC system converges, the level of the modeling signal is reduced to achieve good NR performance. Besides controlling the level of the modeling, the gain control parameter is employed in adjusting the various other parameters too, viz. fixed step-size, regularization parameter, convergence monitoring parameter, while computing the time-varying normalized step-size for the SPM filter. The simulation results demonstrate that the proposed method (equipped with the proposed modifications) outperforms the previous method and yet with a negligible increase in the computational complexity.

1. Introduction

With urbanization and modernization, the acoustic noise pollution has become a serious threat to human health [1]. The noise reduction (NR), for comfortable living, can be achieved either by passive or active means. The passive noise control (PNC) systems employ absorbing materials to "absorb" the unwanted noise by converting it to other form of energy, e.g., heat. The traditional PNC works well for high frequency noise sources; however, does not appear as a viable solution, due to the weight, size, and the cost constraints, for the low frequency acoustic noise [2]. In contrast to PNC (based on absorbing the acoustic noise), the active noise control (ANC) relies on generating an appropriate "anti-noise" signal. The antinoise (canceling) signal is acoustically combined with the noise to be canceled. The destructive interference between the two would result in NR [3]. The research activities in the area of ANC [4,5] have resulted successfully achieving NR in many applications, viz., air conditioning ducts, cars, aircrafts, headphones, and so on (see [6–9] and references therein). The ANC systems are designed to provide NR in a specific region of interest. Essentially, a single-channel scenario can be deployed for NR in a local region, or a multiple-channel scenario when it is desired to cover a large space [4,5]. In this paper, we stick to the single-channel scenario, however, the presented theory and methods can be extended to multiple-channel applications, if needed.

Depending upon the application at hand, the ANC may be implemented in either of two configurations, the feedforward ANC (FFANC) or feedback ANC (FBANC). A reference microphone is available to pick up the reference signal for the ANC adaptive filter in FFANC. The reference microphone cannot be installed due to the physical constraints in many practical scenarios [4,5]. In such cases, it is preferred to employ FBANC comprising one loudspeaker to propagate the canceling signal and an error microphone to pick up the residual error signal. It is worth to mention that FBANC gives plausible performance for the narrowband (predictable) noise sources without requiring any reference signal [4]. Furthermore, it would completely avoid the acoustic feedback which is always present in the case of FFANC due to the coupling between the canceling loudspeaker and the reference microphone [19,20]. See Fig. 1 for a block diagram of the single-channel FBANC, and see Table 1 for listing of various signals and systems in Fig. 1 and the rest of the paper. As shown in Fig. 1, in the absence of the reference

E-mail addresses: muhammad.akhtar@nu.edu.kz, akhtar@ieee.org.

https://doi.org/10.1016/j.dsp.2021.102976

Table 1
Listing of the various mathematical quantities used in the description of signals and systems in this paper.

	$r(n) =$	The reference noise at source
	$d(n) =$	The primary noise disturbance at the error microphone
	$x(n) =$	The reference noise for ANC adaptive filter
	$x_f(n) =$	The filtered-reference or filtered-x signal
	$y(n) =$	The ANC adaptive filter output
	$e(n) =$	The error microphone signal
	$v_0(n) =$	The additive random noise for SPM
	$v(n) =$	The modeling signal for SPM filter
	$D =$	The delay inserted in the path for the modeling signal
Primary Path:	$\boldsymbol{p}(n) =$	$[p_0(n), p_1(n), \cdots, p_{L-1}(n)]^T$
SP:	$\boldsymbol{s}(n) =$	$[s_0(n), s_1(n), \cdots, s_{M-1}(n)]^T$
SPM Filter:	$\hat{\boldsymbol{s}}(n) =$	$[\hat{s}_0(n), \hat{s}_1(n), \cdots, \hat{s}_{M-1}(n)]^T$
ANC adaptive filter:	$\boldsymbol{w}(n) =$	$[w_0(n), w_1(n), \cdots, w_{L-1}(n)]^T$
Reference Signal:	$\boldsymbol{x}(n) =$	$[x(n), x(n-1), \cdots, x(n-L+1)]^T$
Filtered-x Signal:	$\boldsymbol{x}_f(n) =$	$[x_f(n), x_f(n-1), \cdots, x_f(n-L+1)]^T$
Composite SPM Filter:	$\boldsymbol{h}(n) =$	$[\boldsymbol{h}_0^T(n) \quad \boldsymbol{h}_c^T(n)]^T$
	$=$	$[h_0(n), h_1(n), \cdots, h_D(n), \cdots, h_{D+M}(n)]^T$
Modeling Signal:	$\boldsymbol{v}(n) =$	$[\boldsymbol{v}_0^T(n) \quad \boldsymbol{v}_c^T(n)]^T$
	$=$	$[v(n), v(n-1), \cdots, y(n-D-M)]^T$
Note:	Here all acoustic paths and adaptive filters have been assumed to be finite impulse response (FIR) filters.	

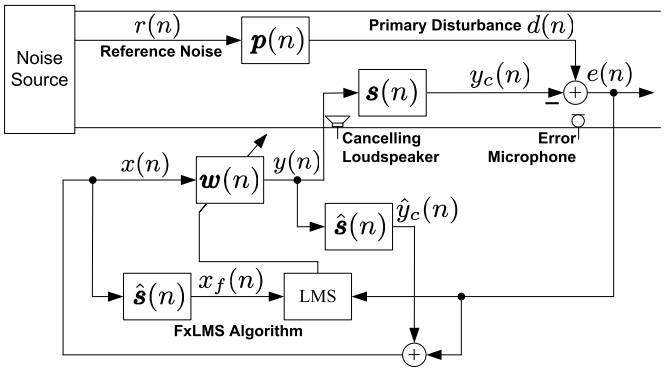

Fig. 1. Block diagram of the FxLMS algorithm-based feedback ANC (FBANC) system.

microphone, the reference signal needs to be generated internally which is achieved by computing an estimate of the cancellation signal and combining it with the error microphone signal.

The most famous adaptive algorithm is the least mean square (LMS) algorithm successfully employed in diverse applications in signal processing, control, and communication [10]. The LMS algorithm can not be directly implemented for ANC applications, due to the so-called (electro-acoustic) secondary path (SP) present between the loudspeaker and the error microphone. The presence of SP requires filtering the reference signal via the SP modeling (SPM) filter. The filtered reference signal is used in the LMS update equation; resulting in the so-called filtered-x LMS (FxLMS) algorithm [5]. The FxLMS algorithm is fairly robust to the errors between the SPM filter and the true SP. It has been shown that the FxLMS algorithm converges with nearly 90° of phase error between the SPM filter and SP [11,12]. Therefore, offline modeling can be used to estimate the SPM filter during an initial training stage for ANC applications [5]. However, SP may be time varying in actual practice and it is desirable to update the SPM filter when ANC is in operation [13]. A variety of approaches have been developed to target adaptation of the SPM filter during operation of the FFANC systems [14–18]. The FBANC system is topic of many recent researches [21–26]. Up to the best knowledge of Author, however, a very little effort has been carried out to investigate the online SPM in FBANC systems [28,27].

The method presented in this paper builds upon the previous work [29]. Here the main objective is to realize improved performance from the view points of NR as well as adaptation of the SPM filter. As in the previous method, the proposed method comprises two adaptive filters which are updated simultaneously. The ANC adaptive filter is updated using the classical FxLMS algorithm [5], and its job is to perform the noise cancellation. The SPM filter identifies the characteristics of the unknown SP, and acts as a supporting filter for the main ANC adaptive filter. The SPM filter is excited by an additive random noise and is adapted using a delay-based adaptive algorithm with a time-varying step-size. A delay is appended in the path of the additive noise before being sent to the SP via the loudspeaker. The initial coefficients in the SPM filter thus attempt to model the appended delay, and the rest of coefficients are used to identify the acoustic SP. The convergence of the coefficients, modeling the appended delay, is used to monitor the convergence status of the SPM filter, as well as regulate the additive random noise injected for SPM. The additive random noise is regulated to have a large-level modeling signal during the transient state of the FBANC system to achieve fast convergence. However, the additive random noise appears around the location of the error microphone and degrades the NR performance. Therefore, injection of the random noise must be removed (or at least reduced) at the steady-state. This, however, also means that the SPM filter will be excited by a low-level modeling signal slowing down its convergence speed [29]. This sluggish convergence issue has been addressed in the proposed method where the step-size in the SPM filter is increased in proportion to reduction in the level of the additive random signal.

The organization of the rest of the paper is as follows. Section 2 gives a brief overview of the FBANC systems, and details exiting work on online SPM in FBANC. Section 3 describes the proposed method, and Section 4 details the numerical results. Finally, a few concluding remarks are presented in Section 5. A short version of this paper was presented at a conference [30].

2. Classical ANC systems

2.1. Feedback ANC (FBANC) systems

Let us consider Fig. 1 which shows a block diagram for the single-channel FBANC systems. Here, the error microphone signal $e(n)$ is given as

$$e(n) = d(n) - y_c(n), \tag{1}$$

where $y_c(n) = \boldsymbol{c}^T(n)\boldsymbol{y}(n)$ is the cancellation signal for the primary noise $d(n)$ and where T denotes the transposition operation. It is important to notice that $e(n)$ is directly available via the error microphone and $d(n)$ is not accessible. Furthermore, the information about the reference noise $r(n)$ is not available due to the absence of any reference microphone. Therefore, the error signal $e(n)$ is not only used to update the coefficients of the ANC adaptive filter, but also to generate the reference signal $x(n)$ well correlated with the disturbance signal $d(n)$. The latter is achieved by filtering the output $y(n)$ the ANC adaptive filter $\boldsymbol{w}(n)$ via one copy of the SPM filter $\hat{\boldsymbol{s}}(n)$ and combining with the error signal $e(n)$ as

$$\begin{aligned} x(n) &= e(n) + \hat{\boldsymbol{c}}^T(n)\boldsymbol{y}(n) \\ &= d(n) + \left[\hat{\boldsymbol{s}}(n) - \boldsymbol{s}(n)\right]^T \boldsymbol{y}(n), \end{aligned} \tag{2}$$

which shows that if $\hat{\boldsymbol{s}}(n) \approx \boldsymbol{s}(n)$ (available from offline system identification [4], for example), then $x(n) \approx d(n)$. Using the same error signal $e(n)$, the FxLMS algorithm updates the coefficients of the ANC adaptive filter $\boldsymbol{w}(n)$ as [4]

$$\boldsymbol{w}(n+1) = \boldsymbol{w}(n) + \mu_w e(n)\boldsymbol{x}_f(n), \tag{3}$$

where μ_w denotes the step-size parameter, and $\boldsymbol{x}_f(n)$ is a vector for the filtered-x signal $x_f(n)$ which is computed as

$$x_f(n) = \hat{\boldsymbol{c}}^T(n)\boldsymbol{x}(n), \tag{4}$$

where $\boldsymbol{x}(n)$ is comprised of samples of $x(n)$ (see Table 1). It is worth to mention that the true SP $\boldsymbol{s}(n)$ may be time varying in many practical situations. In order to ensure $\hat{\boldsymbol{s}}(n) \approx \boldsymbol{s}(n)$ during all operating conditions, the SPM filter $\hat{\boldsymbol{s}}(n)$ needs to be updated during the operation of ANC system, as considered in this paper.

2.2. Basic method for SPM in FBANC systems

The basic method for online SPM in FBANC systems [28] is a direct extension of that described in [14] for the FFANC systems. The method in [28] adds a few heuristically selected thresholds though. In this paper, a simplified version (as developed in [27]) is briefly reviewed. The block diagram of the basic method is shown in Fig. 2, where the additive random noise $v_0(n)$ is used to generate the modeling signal $v(n)$. The modeling signal $v(n)$ is mixed with the ANC adaptive filter output $y(n)$ to give a composite signal for the canceling loudspeaker as

$$u(n) = y(n) - v(n), \tag{5}$$

and hence, the residual error signal at the error microphone can now be expressed as

$$\begin{aligned} e(n) &= d(n) - u_c(n), \\ &= d(n) - \boldsymbol{c}^T(n)(\boldsymbol{y}(n) - \boldsymbol{v}(n)), \\ &= d(n) - \boldsymbol{c}^T(n)\boldsymbol{y}(n) + \boldsymbol{c}^T(n)\boldsymbol{v}(n). \end{aligned} \tag{6}$$

Using $e(n)$ as a 'desired' response for adaptation of the SPM filter $\hat{\boldsymbol{s}}(n)$, the corresponding error signal $e_c(n)$ is generated as

$$\begin{aligned} e_c(n) &= e(n) - \hat{\boldsymbol{c}}^T(n)\boldsymbol{y}(n), \\ &= \left[d(n) - \boldsymbol{c}^T(n)\boldsymbol{y}(n)\right] + \left[\boldsymbol{s}(n) - \hat{\boldsymbol{s}}(n)\right]^T \boldsymbol{v}(n). \end{aligned} \tag{7}$$

It is interesting to note that the first term on the right-hand-side (RHS) of (7) is 'error signal' for adaptation of the ANC adaptive filter $\boldsymbol{w}(n)$, and the second term carries information for adaptation of the SPM filter $\hat{\boldsymbol{s}}(n)$. Therefore, both adaptive filters $\boldsymbol{w}(n)$ and $\hat{\boldsymbol{s}}(n)$ are updated using the same error signal $e_c(n)$. The coefficients

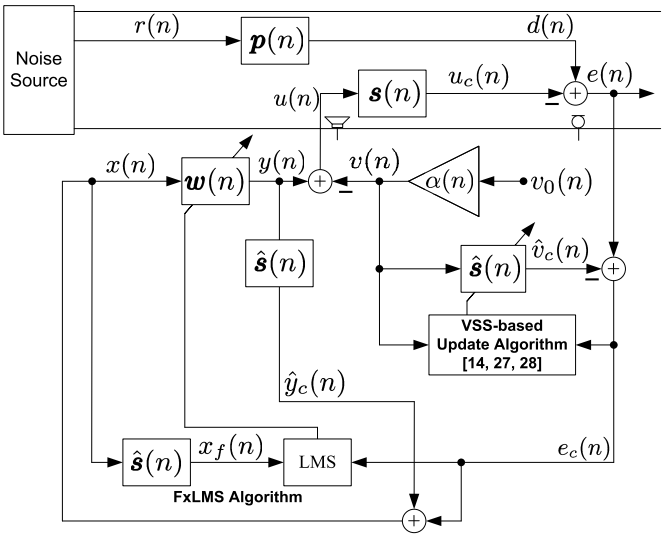

Fig. 2. Block diagram of the basic method for FBANC systems with online SPM.

of the SPM filter $\hat{\boldsymbol{s}}(n)$ are updated using a variable step-size (VSS)-based adaptive algorithm [14] as

$$P_e(n) = \lambda P_e(n-1) + \gamma e^2(n), \tag{8a}$$

$$P_{e_c}(n) = \lambda P_{e_c}(n-1) + \gamma e_c^2(n), \tag{8b}$$

$$\alpha(n) = P_{e_c}(n)/P_e(n), \tag{8c}$$

$$\mu_c(n) = \alpha(n)\mu_1 + (1-\alpha(n))\,\mu_2;\ (\mu_1 < \mu_2), \tag{8d}$$

$$\hat{\boldsymbol{c}}(n+1) = \hat{\boldsymbol{s}}(n) + \mu_c(n)e_c(n)\boldsymbol{v}(n), \tag{8e}$$

where $P_e(n)$ and $P_{e_c}(n)$ denote (lowpass) power estimates of the error signals $e(n)$ and $e_c(n)$, respectively, $0 \ll \lambda < 1$ and $0 < \gamma \ll 1$ are parameters for the lowpass estimators in (8a) and (8b), $\alpha(n)$ in (8c) is a time-varying parameter to compute the VSS $\mu_c(n)$ in (8d), and (8e) is LMS-update equation for adapting the SPM filter $\hat{\boldsymbol{s}}(n)$. It can be shown that $\alpha(n) \approx 1$ at the start-up and $\alpha(n)$ reduces as the ANC system converges (see [14] for details). The parameter $\alpha(n)$ is, therefore, used to control the level of the additive random signal $v_0(n)$ as follows

$$v(n) = \alpha(n)v_0(n), \tag{9}$$

which results in the modeling signal $v(n) = v_0(n)$ at the start-up and the level of modeling signal $v(n)$ decreases as the ANC system converges. This improves the NR performance, as the last term on the RHS of (6) becomes small. On the other hand, a low-level modeling signal $v(n)$ would slow down the convergence speed of the SPM filter $\hat{\boldsymbol{s}}(n)$ (see (8e)). This degradation in the convergence of SPM filter is somewhat compensated by increasing the step-size $\mu_c(n)$ in (8d). The coefficients of the ANC adaptive filter $\boldsymbol{w}(n)$ are updated using the FxLMS algorithm (3) using the error signal $e_c(n)$ as

$$\boldsymbol{w}(n+1) = \boldsymbol{w}(n) + \mu_w e_c(n)\boldsymbol{x}_f(n). \tag{10}$$

3. Proposed method for SPM in FBANC systems

Block diagram of the proposed method is shown in Fig. 3, where the gain-controlled modeling signal $v(n)$ is computed as

$$v(n) = \rho(n)v_0(n), \tag{11}$$

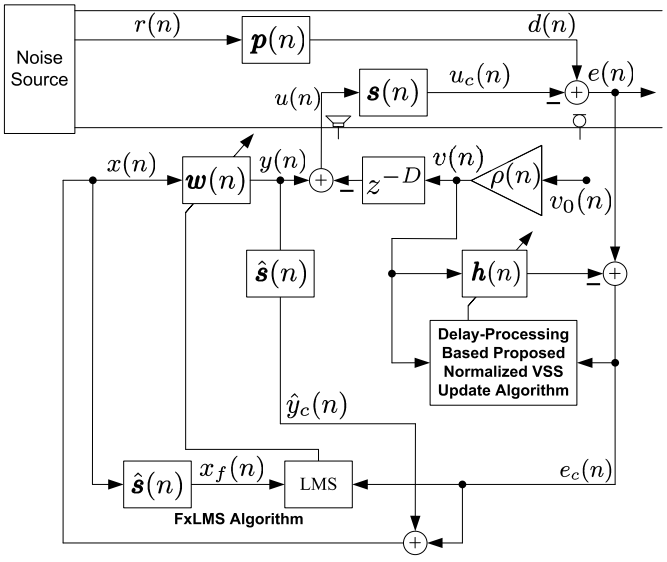

Fig. 3. The proposed method for the FBANC systems with online SPM.

where $\rho(n)$ is the gain control parameter. The role of $\rho(n)$ is similar to that of the parameter $\alpha(n)$ in the basic method, and therefore, it is desired to have $\rho(0) = 1$ and $\rho(n) \to 0$ as $n \to \infty$ (the computation of such $\rho(n)$ in the proposed method is explained later). The loudspeaker signal $u(n)$ in the proposed method is computed as

$$u(n) = y(n) - v(n - D), \tag{12}$$

where D denotes the delay inserted in the path for the modeling signal $v(n)$ (see block z^{-D} in Fig. 3), and $y(n)$ is the output signal of the ANC adaptive filter $\boldsymbol{w}(n)$ computed as

$$y(n) = \boldsymbol{w}^T(n)\boldsymbol{x}(n). \tag{13}$$

The inserted delay increases the effective path traversed by the modeling signal $v(n)$. Therefore, the SPM filter $\boldsymbol{h}(n)$ is a composite filter comprising two parts $\boldsymbol{h_0}(n)$ and $\boldsymbol{h}_c(n)$ (see Table 1). The initial coefficients $\boldsymbol{h_0}(n)$ model the inserted delay, and latter coefficients attempt to identify the SP $\boldsymbol{s}(n)$. The coefficients of 'delay-based' composite SPM filter $\boldsymbol{h}(n)$ are updated using the normalized LMS (NLMS) algorithm [31] as

$$\boldsymbol{h}(n+1) = \boldsymbol{h}(n) + \mu_h(n)\frac{e_c(n)\boldsymbol{v}(n)}{||\boldsymbol{v}(n)||_2^2 + \epsilon}, \tag{14}$$

where $||\cdot||_2$ denotes the Euclidean norm, ϵ is the regularization parameter (a small positive constant to avoid division by zero), $\mu_h(n)$ is the normalized variable step-size (VSS), and $e_c(n)$ is the (adaptation) error signal. The error microphone signal $e(n) = d(n) - u_c(n)$ is combined with the output of the SPM filter $\boldsymbol{h}(n)$ to give $e_c(n)$ as

$$\begin{aligned} e_c(n) &= e(n) - \boldsymbol{h}^T(n)\boldsymbol{v}(n) \\ &= [d(n) - \boldsymbol{c}^T(n)\boldsymbol{y}(n)] + [\boldsymbol{c}^T(n)\boldsymbol{v}(n-D) - \boldsymbol{h}^T(n)\boldsymbol{v}(n)]. \end{aligned} \tag{15}$$

It is evident from the second term $[\boldsymbol{c}^T(n)\boldsymbol{v}(n-D) - \boldsymbol{h}^T(n)\boldsymbol{v}(n)]$ on the RHS of (15) that $\boldsymbol{h}(n)$ needs to take care of the inserted delay as well as to estimate the true SP $\boldsymbol{s}(n)$ to ensure that $[\boldsymbol{c}^T(n)\boldsymbol{v}(n-D) - \boldsymbol{h}^T(n)\boldsymbol{v}(n)] \to 0$ as $n \to \infty$. The normalized VSS $\mu_h(n)$ in (14) is computed as

$$\mu_h(n) = \begin{cases} \dfrac{\hat{\mu}\hat{N}_D(n)}{P_{e_c}(n) + \epsilon}; & \dfrac{\hat{N}_D(n)}{P_{e_c}(n)} > \mu_{h_{\min}} \\ \mu_{h_{\min}}; & \text{otherwise} \end{cases} \tag{16}$$

where $\hat{\mu}$ is a (semi-) fixed step-size parameter, $P_{e_c}(n)$ estimates power of $e_c(n)$ as in (8b), $\mu_{h_{\min}}$ is the empirically selected minimum value for $\mu_h(n)$, and $\hat{N}_D(n)$ is a parameter computed as

$$\hat{N}_D(n) = \lambda\hat{N}_D(n-1) + \gamma\frac{\left(||\boldsymbol{h_0}(n)||_2^2||\boldsymbol{v}_{\boldsymbol{0}}^T(n)||_2^2\right)}{\rho(n)D}, \tag{17}$$

where $\rho(n)$ is the same parameter as used in computing the modeling signal $v(n)$. Since the NLMS algorithm spreads the error among the filter coefficients [31], the convergence of $\boldsymbol{h_0}(n)$ (for which the desired solution is known a priori) can be used to monitor the convergence status of the composite SPM filter $\boldsymbol{h}(n)$. Essentially, we compute the parameter $\rho(n)$ using coefficients of $\boldsymbol{h_0}(n)$ as

$$\rho(n) = \frac{\sum_{i=0}^{D-1}|h_i(n)|^2}{D}. \tag{18}$$

By initializing $\boldsymbol{h_0}(0) = \boldsymbol{1}$ (vector of all 1's), it is straightforward to conclude that $\rho(0) = 1$ initially and $\rho(n) \to 0$ as the ANC system converges at $n \to \infty$.

The second term on the RHS of (15) represents the error signal required for adaptation of the SPM filter. As $\boldsymbol{h}(n)$ converges, it is expected $[\boldsymbol{c}^T(n)\boldsymbol{v}(n-D) - \boldsymbol{h}^T(n)\boldsymbol{v}(n)] \to 0$, and hence $e_c(n) \to [d(n) - \boldsymbol{c}^T(n)\boldsymbol{y}(n)]$. Therefore, $e_c(n)$ is used (as $e(n)$ in (2)) to generate the reference signal $x(n)$ as

$$\begin{aligned} x(n) &= e_c(n) + \hat{\boldsymbol{c}}^T(n)\boldsymbol{y}(n), \\ &\approx [d(n) - \boldsymbol{c}^T(n)\boldsymbol{y}(n)] + \hat{\boldsymbol{c}}^T(n)\boldsymbol{y}(n), \\ &\approx d(n). \end{aligned} \tag{19}$$

Using the same error signal $e_c(n)$ (14) the coefficients of the ANC adaptive filter $\boldsymbol{w}(n)$ are updated by employing the FxLMS algorithm as in (10).

3.1. Convergence monitoring

The inserted delay D results in requiring an *extended-length* composite filter $\boldsymbol{h}(n)$ for modeling of SP. This obviously increases the computational complexity. However, the delay-based adaptation results in designing a parameter $\rho(n)$ which serves two purposes. First, $\rho(n)$ regulates the modeling signal $v(n)$ (11) such that the modeling signal is reduced as the ANC system converges. Second, $\rho(n)$ helps in designing a strategy for convergence monitoring and detection of a sudden change in SP (as given in Table 2 and explained below).

Table 2 presents an algorithm for the convergence monitoring. The threshold $T1$ (on $\rho(n)$) can be selected as a small number less than unity, indicating that ANC system is converging. $T2$ is a dynamic threshold which is updated as long as $\rho(n)$ keeps on decreasing. When $\rho(n)$ approaches its steady-state, the `FLAG1` is set (`TRUE`); and the algorithm starts monitoring for any sudden changes in the acoustic paths. In such a situation of a change, the SPM filter error $e_c(n)$ would suddenly increase. This results in a drop in the value of $\mu_h(n)$ (the normalized VSS in (16)) which is computed inversely proportional to $P_{e_c}(n)$ (power estimate of the error signal $e_c(n)$). Once $\mu_h(n)$ drops below a pre-decided empirical value $\mu_{h_{\min}}$, the coefficients $\boldsymbol{h_0}(n)$ are reset to all 1's. This results in $\rho(n) = 1$ (18) which in turn makes $v(n) = v_0(n)$ (11), i.e., a large-level modeling signal is injected for fast a re-convergence of the SPM filter $\boldsymbol{h}(n)$.

Table 2
Algorithm for convergence monitoring of the SPM filter and SP-change detection in the proposed method.

	`FLAG1 = FALSE` % Change Detection Flag
	`FLAG2 = FALSE` % Convergence Monitoring Flag
	$0 < \texttt{T1} \ll 1, \texttt{T2}$ % Thresholds on $\rho(n)$
1.	**if** `FLAG1 == FALSE`
2.	**if** `FLAG2 == FALSE`
3.	Update $\hat{\mu}$ in (16) as $\hat{\mu} \leftarrow \hat{\mu}/\rho(n)$
4.	Update ϵ in (16) as $\epsilon \leftarrow \rho(n)$
5.	**if** $\rho(n) \leq \texttt{T1}$
6.	Update threshold on $\rho(n)$ as $\texttt{T2} = \rho(n)$
7.	Reset convergence monitoring flag as `FLAG2 = TRUE`
8.	**end**
9.	**elseif** `FLAG2 == TRUE`
10.	**if** $\rho(n) \leq \texttt{T2}$
11.	Update threshold on $\rho(n)$ as $\texttt{T2} = \rho(n)$
12.	**else**
13.	Reset change detection flag as `FLAG1 = TRUE`
14.	**end**
15.	**elseif** `FLAG1 == TRUE`
16.	**if** $\mu_h(n) < \mu_{h_{\min}}$
17.	Re-initialize $\boldsymbol{h_0}(n)$ to all 1's resulting in $\rho(n) = 1$
18.	Reset flags `FLAG1= FALSE`, `FLAG2= FALSE`, and running threshold `T2`
19.	**end**
20.	**end**

Table 3
Summary of the proposed method.

Available:
The error microphone signal $e(n)$
Internally generated additive random noise $v_0(n)$

Parameters and Initialization:
L, M, D, λ, γ, ϵ, $\mu_{h_{\min}}$, $\hat{\mu}$, μ_w
$\boldsymbol{w}(n) = \boldsymbol{0}_{L\times 1}$, $\boldsymbol{x}(n) = \boldsymbol{0}_{L\times 1}$, $\boldsymbol{h}(n) = \boldsymbol{0}_{(M+D)\times 1}$

Computations:
$v(n) = v_0(n)$; % Initially assume $\rho(n) = 1$
while $\{e(n)\}$ available *do* $\cdots$
1. Update the secondary path modeling filter $\boldsymbol{h}(n)$:
$\boldsymbol{v}(n) = [v(n), v(n-1), \cdots, y(n-D-M)]^T$; % Update modeling signal vector
$e_c(n) = e(n) - \boldsymbol{h}^T(n)\boldsymbol{v}(n)$; % Adaptation error signal $e_c(n)$
$P_{e_c}(n) = \lambda P_{e_c}(n-1) + \gamma e_c^2(n)$; % Estimate power of $e_c(n)$
$\hat{N}_D(n) = \lambda \hat{N}_D(n-1) + \gamma \dfrac{\left(||\boldsymbol{h_0}(n)||_2^2 ||\boldsymbol{v_0}^T(n)||_2^2\right)}{\rho(n)D}$; % convergence status of $\boldsymbol{h}(n)$
$\mu_h(n) = \begin{cases} \dfrac{\hat{\mu}\hat{N}_D(n)}{P_{e_c}(n)+\epsilon}; & \dfrac{\hat{N}_D(n)}{P_{e_c}(n)} > \mu_{h_{\min}} \\ \mu_{h_{\min}}; & \text{otherwise} \end{cases}$; % Normalized VSS for $\boldsymbol{h}(n)$
$\boldsymbol{h}(n+1) = \boldsymbol{h}(n) + \mu_h(n)\dfrac{e_c(n)\boldsymbol{v}(n)}{||\boldsymbol{v}(n)||_2^2 + \epsilon}$; % Update coefficient of $\boldsymbol{h}(n)$
2. Update the ANC adaptive filter $\boldsymbol{w}(n)$:
$y(n) = \boldsymbol{w}^T(n)\boldsymbol{x}(n)$; % ANC adaptive filter output
$x(n) = e_c(n) + \hat{\boldsymbol{c}}^T(n)\boldsymbol{y}(n)$; % Estimate reference signal
$x_f(n) = \hat{\boldsymbol{c}}^T(n)\boldsymbol{x}(n)$; % Compute filtered-x signal
$\boldsymbol{x}_f(n) = [x_f(n), x_f(n-1), \cdots, x_f(n-L+1)]^T$; % Update filtered-x vector
$\boldsymbol{w}(n+1) = \boldsymbol{w}(n) + \mu_w e_c(n)\boldsymbol{x}_f(n)$; % FxLMS algorithm for $\boldsymbol{w}(n)$
$\boldsymbol{x}(n) = [x(n), x(n-1), \cdots, x(n-L+1)]^T$; % Update reference signal vector
3. Compute the loudspeaker signal:
$\rho(n) = \dfrac{\sum_{i=0}^{D-1} |h_i(n)|^2}{D}$; % Gain-control parameter
$v(n) = \rho(n)v_0(n)$; % modeling signal
$u(n) = y(n) - v(n-D)$; % loudspeaker signal
4. Execute convergence monitoring and change detection algorithm in Table 2.
end while

The parameter $\rho(n)$ converges to (ideally) zero at the steady-state, which makes $v(n)$ very small. This makes convergence of $\boldsymbol{h}(n)$ (14) very slow as indeed observed in the previous method [29]. In order to compensate such effect two modifications are suggested while computing the normalized VSS $\mu_h(n)$. The parameter $\hat{N}_D(n)$ computed using coefficients $\boldsymbol{h_0}(n)$ and corresponding signal vector $\boldsymbol{v_0}(n)$ (see (17)) is made inversely proportional to $\rho(n)$. Furthermore, the fixed step-size $\hat{\mu}$ is also varied inversely proportional to $\rho(n)$ (see line 3 in Table 2). Yet another modification is suggested to update the regularization parameter ϵ in (16) using $\rho(n)$ during the initial stage of convergence (see line 4 in Table 2). These modifications substantially improve the NR performance and the modeling accuracy of the SPM filter, as demonstrated by detailed simulation results presented later.

3.2. Summary of proposed method and computational complexity analysis

The execution summary (in a pseudo code style) of the proposed method is given in Table 3. The two adaptive filters $\boldsymbol{w}(n)$ and $\boldsymbol{h}(n)$ can be initialized by the null vectors of appropriate lengths. At the star-up, it is assumed that $\rho(n) = 1$, and hence $v(n) = v_0(n)$. Furthermore, the reference signal vector $\boldsymbol{x}(n)$ is initialized as a null vector, as the reference signal $x(n)$ is computed later internally and not available directly.

The computational complexity analysis can be performed on the basis of computations required per iteration of the algorithm. Using the computations give in Section 2.2, it is straightforward to see that the basic method for FBANC with online SPM [27] would require $2L + 4M + 13$ multiplications, $2L + 4M + 3$ additions, and one division per iteration of the algorithm, where L is the length of the FIR ANC adaptive filter $\boldsymbol{w}(n)$ and M is the length of the FIR SPM filter $\hat{\boldsymbol{s}}(n)$. The proposed method is based on a few modifications to the previous method (see Section 3.1, and Tables 2 and 3).

Using the summary given in Tables 2 and 3, and ignoring the modifications highlighted in Section 3.1, the previous method would require $2L+5M+6D+11$ multiplications, $2L+4M+3D+1$ additions, and 3 division per iteration. In addition to the computations required for the previous method [29], the proposed method would require one extra multiplication (in the denominator of $\hat{N}_D(n)$) and one extra division in updating the step-size $\hat{\mu}$ (see Table 2). In summary, the computational complexity of the previous method is somewhat higher than that of the basic method, and that the computational requirements of the proposed method are similar to that of the previous method.

4. Numerical results

This section presents detailed numerical results to evaluate the performance of various methods discussed in this paper. The simulations have been designed to mimic the practical scenarios. The first objective is to develop understanding of the effect of the modeling error (between the true acoustic SP $\boldsymbol{s}(n)$ and the SPM filter $\hat{\boldsymbol{s}}(n)$) on the performance of the conventional FBANC systems. The second and the main objective is to use these results to demonstrate improved performance of the proposed method for the FBANC systems. The reference noise comprises pure sinusoids of frequencies 165 Hz, 290 Hz, 315 Hz, 410 Hz, and 600 Hz. The sampling frequency is 4 kHz, and the measurement noise is added with 30 dB single-to-noise ratio (SNR). The results presented are ensemble averaged over 25 realizations. The data for the acoustic paths $\boldsymbol{p}(n)$ and $\boldsymbol{s}(n)$, modeled as FIR filters of length 256 and 128, respectively, are taken from the disk provided with [4]. The impulse response characteristics of the primary and secondary acoustic paths are shown in Fig. 4, and the corresponding magnitude and phase responses are shown in Fig. 5.

The performance comparison has been carried out on the basis of the NR achieved around the location of the error microphone, which is computed as

$$\mathrm{NR}(n) = 10\log_{10}\frac{E\left\{e^2(n)\right\}}{E\left\{d^2(n)\right\}}(\mathrm{dB}). \tag{20}$$

It is also very important to compute the modeling accuracy which signifies the normalized misalignment (NM) between the true SP $\boldsymbol{s}(n)$ and the SPM filter $\hat{\boldsymbol{s}}(n)$. The NM measure is computed as

$$\mathrm{NM}(n) = 10\log_{10}\frac{\|\boldsymbol{s}(n) - \hat{\boldsymbol{s}}(n)\|_2^2}{\|\boldsymbol{s}(n)\|_2^2}(\mathrm{dB}). \tag{21}$$

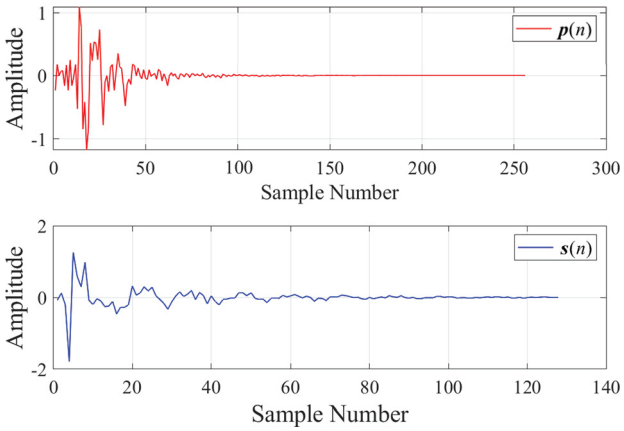

Fig. 4. Impulse response characteristics of the acoustic paths used in the computer simulations.

4.1. Effect of modeling error on the conventional FBANC systems

Let us first study the effect of the modeling error between $\boldsymbol{s}(n)$ and $\hat{\boldsymbol{s}}(n)$ on the performance of the conventional FBANC system. The ANC adaptive filter $\boldsymbol{w}(n)$ is an FIR filter of length $L = 192$ and is initialized by a null vector of same length $L = 192$. The corresponding step-size parameter is adjusted to $\mu_w = 1 \times 10^{-6}$. The length of the SPM filter $\hat{\boldsymbol{s}}(n)$ is same as that of the SP $\boldsymbol{s}(n)$, i.e., $M = 128$. The effect of the modeling error on the performance of the FFANC systems has been studied in [13]. We follow a similar approach here for the conventional FBANC system as shown in Fig. 1. The experiments have been performed for various versions of $\hat{\boldsymbol{s}}(n)$ in Fig. 1. These variants of $\hat{\boldsymbol{s}}(n)$ have been generated by replacing the last coefficients of the true impulse response $\boldsymbol{s}(n)$ (shown in Fig. 4) with zeros. The curves for mean NR in the conventional FBANC system are shown in Fig. 6, where the legend shows the number of last zero-valued samples in $\hat{\boldsymbol{s}}(n)$. Thus "0" indicates the ideal scenario that the true acoustic SP $\boldsymbol{s}(n)$ and the SPM filter $\hat{\boldsymbol{s}}(n)$ are having exactly the same coefficients, i.e., $\hat{\boldsymbol{s}}(n) = \boldsymbol{s}(n)$. On the other hand, the number "125" in the legend of Fig. 6 shows that only first three samples in the SPM filter $\hat{\boldsymbol{s}}(n)$ are exactly same as those in the impulse response of the true $\boldsymbol{s}(n)$, whereas the last 125 coefficients have been replaced with zeros. This simple experiment demonstrates that the modeling error between $\boldsymbol{s}(n)$ and $\hat{\boldsymbol{s}}(n)$ indeed affects the NR performance of the conventional FBANC systems. In order to signify the initial convergence trend of various curves, the curves in Fig. 6(a) are replotted in Fig. 6(b) using a log-scale for the x-axis.

In the next experiment, we study the influence of the modeling error from another perspective. Let us assume that at the start-up of ANC system the SP has been exactly identified using some offline measurements, i.e., $\hat{\boldsymbol{s}}(n) = \boldsymbol{s}(n)$. At the middle of operation of ANC system, the true SP changes to a new value, which may happen in many practical situation, for example, moving noise sources, bringing some object to the close proximity of FBANC system, position change of portable ANC devices like NR headsets/hearing aids, etc. Such situation would result mainly in the change of gain characteristic, as observed for acoustic path in hearing aids [32]. A few examples for such characteristics are plotted in Fig. 7, where the legend shows the gain drop (on a linear scale). Here gain equal to 1 corresponds to the original path characteristics as shown in Fig. 5(a). The experiments are performed for the conventional FBANC system of Fig. 1 by considering that $\hat{\boldsymbol{s}}(n) = \boldsymbol{s}(n)$ at the start-up. The true SP changes to as shown in Fig. 7, whereas there is no way to update the coefficients of $\hat{\boldsymbol{s}}(n)$, and hence the modeling error suddenly increases during the middle of simulation. The change in the primary path $\hat{\boldsymbol{p}}(n)$ is simulated by reversing sign of its coefficients. The simulation results for these experiments are

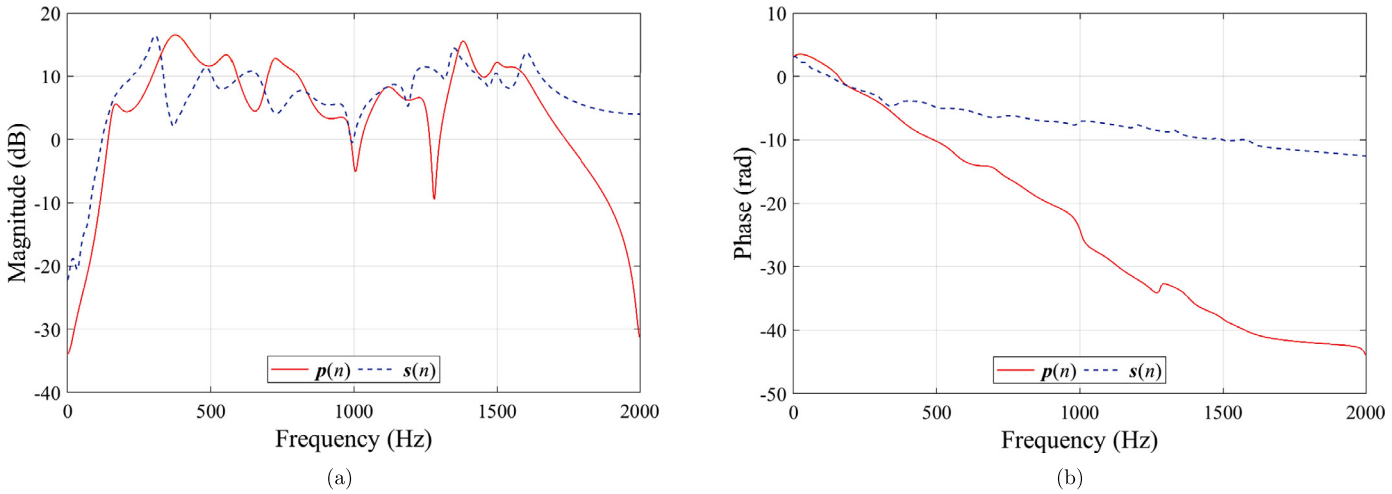

Fig. 5. The magnitude response (a) and the phase response (b) characteristics of the acoustic paths used in computer simulations.

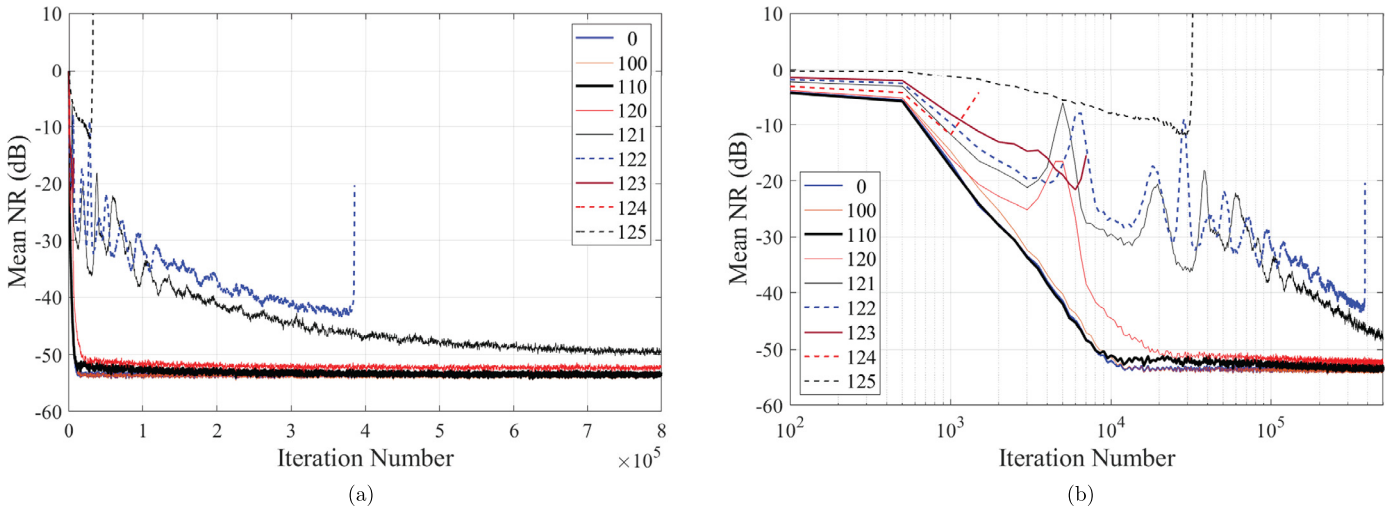

Fig. 6. Studying the influence of the imperfect secondary path modeling filter on the noise reduction performance of the standard FBANC system. (The curves in (a) are replotted in (b) using log-scale for the x-axis.)

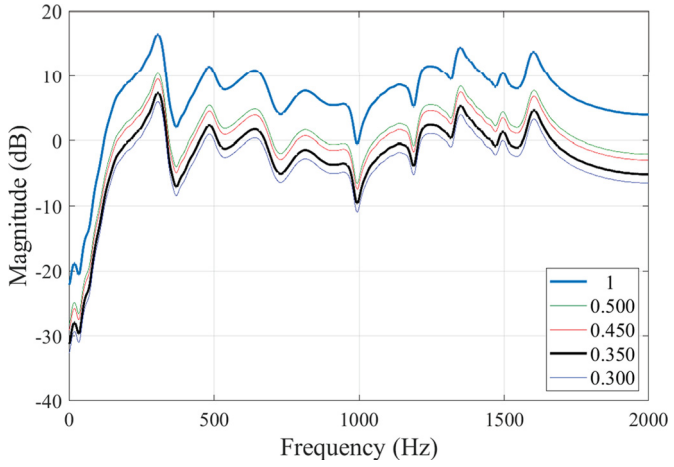

Fig. 7. Magnitude response characterless of the secondary path under various gain conditions.

shown in Fig. 8 (a) and (b), where (b) shows a zoomed version of curves in (a) around the point of change.

From the above-detailed experiments and the corresponding results presented in Figs. 6–8, it is observed that the FxLMS algorithm-based conventional FBANC system is fairly robust to the modeling errors between $\boldsymbol{s}(n)$ and $\hat{\boldsymbol{s}}(n)$. Therefore, offline modeling can be used to estimate $\boldsymbol{s}(n)$ during an initial training stage for the ANC applications [5]. However, NR performance degrades if the SPM filter $\hat{\boldsymbol{s}}(n)$ does not match well enough with the true SP $\boldsymbol{s}(n)$. For some applications, the true SP may be time varying which in general may result in a NR performance inferior to that under the ideal conditions. In the worst case scenario, the whole FBANC system may become unstable. Accordingly, we should use online identification of the SP characteristics to ensure the stability and to maintain the NR performance when the SP is time varying. Therefore, it is desirable to estimate the SP online when the ANC is in operation [13].

4.2. Choosing delay D in the proposed method

It is very important to choose an appropriate value of the delay D (see block z^{-D} in Fig. 3) in the proposed method. As explained earlier, the key objective of inserting this delay is to have information about the convergence status of the (composite) SPM filter $\boldsymbol{h}(n)$. With the understanding that the initial coefficients of $\boldsymbol{h}(n)$ would attempt to model the inserted delay and with the knowledge that the adaptive algorithm would spread the approximation error to all coefficient [31]; the initial coefficients of $\boldsymbol{h}(n)$ indeed

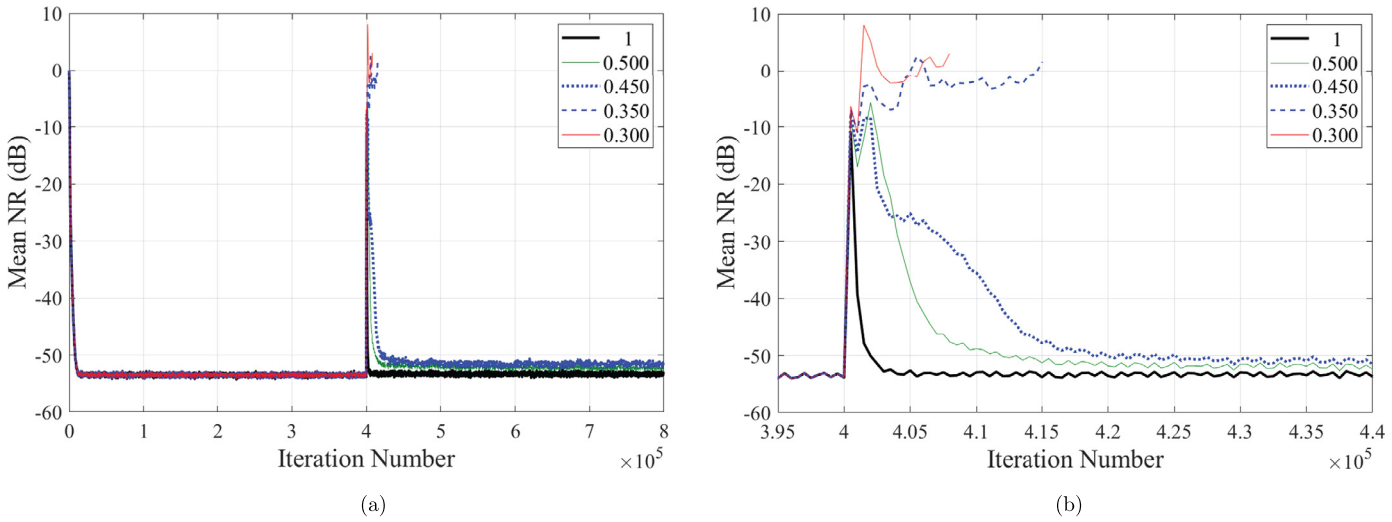

Fig. 8. Studying the influence of modeling error on the noise reduction performance of the standard FBANC system when the true acoustic paths change suddenly to a new characteristic (as shown in Fig. 7) during the middle of simulation. (The zoomed version of curves around the point of change is given in (b).)

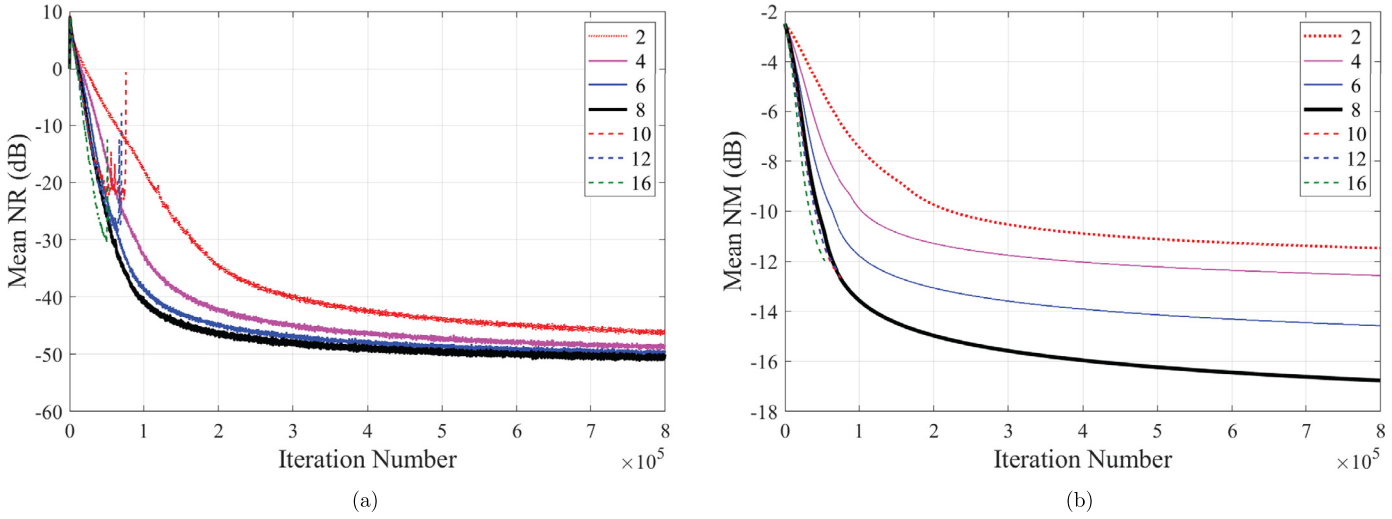

Fig. 9. Experiments for the proposed method with various values of the inserted delay D. (a) Mean noise reduction (NR) (in dB), and (b) Mean normalized misalignment (NM) (in dB).

give information about the convergence status of the overall composite filter $\boldsymbol{h}(n)$. It is important to mention that a (too) small value for D would result in errors in the judgment about the convergence status of the overall filter, whereas a (too) large value would result in an increased computational complexity. Therefore, it is a trade-off situation. In order to get further insight, experiments have been performed to study the impact of selecting an appropriate delay for the proposed method. The reference signal is the same as described earlier, and the acoustic paths are same as shown in Fig. 5. It is assumed that an initial estimate of the SPM filter (with the modeling error of about -2.5 dB) is available from some offline system identification experiments.

The performance of the proposed method for various values of the delay D is shown in Fig. 9(a) and (b). Here, legends show values of the delay D used in simulations. It is important to recall here that the gain-control parameter $\rho(n)$ for the modeling signal is computed using the initial coefficients of $\boldsymbol{h}(n)$ (see (18)). Therefore, a small value for the delay D would mean a small length of the composite SPM filter $\boldsymbol{h}(n)$. This would quickly reduce the modeling signal $v(n)$ (see (11)) which would in turn make the convergence of $\boldsymbol{h}(n)$ sluggish. This in turn degrades the convergence of FxLMS-based ANC adaptive filter $\boldsymbol{w}(n)$ and hence the overall NR performance. Increasing the value of the delay D would increase the length of $\boldsymbol{h}(n)$ which affects its convergence speed. Now $\rho(n)$ stays high for a somewhat longer time as compared with the situation described earlier. This improves the accuracy of the SPM filter $\boldsymbol{h}(n)$ which in turn improves the efficiency of the NR process comprising the ANC adaptive filter $\boldsymbol{w}(n)$. Further increase in the delay D increases computational complexity of $\boldsymbol{h}(n)$ and affects its convergence speed. This in turns degrades the NR performance. Since both $\boldsymbol{h}(n)$ and $\boldsymbol{w}(n)$ are adapted using the same error signal $e_c(n)$, the overall ANC system may become unstable. Our experience shows that $D = 8$ is a good choice from the view points of computational complexity and stable convergence.

4.3. Performance comparison for stationary acoustic environment

In the numerical results presented in this section, the following methods have been considered for the performance comparison:

1. The main objective of any ANC system is to provide NR around some desired location. The conventional FBANC system shown in Fig. 1 would give the best NR performance, provided that SPM filter $\hat{\boldsymbol{s}}(n)$ perfectly matches the unknown SP $\boldsymbol{s}(n)$. Since

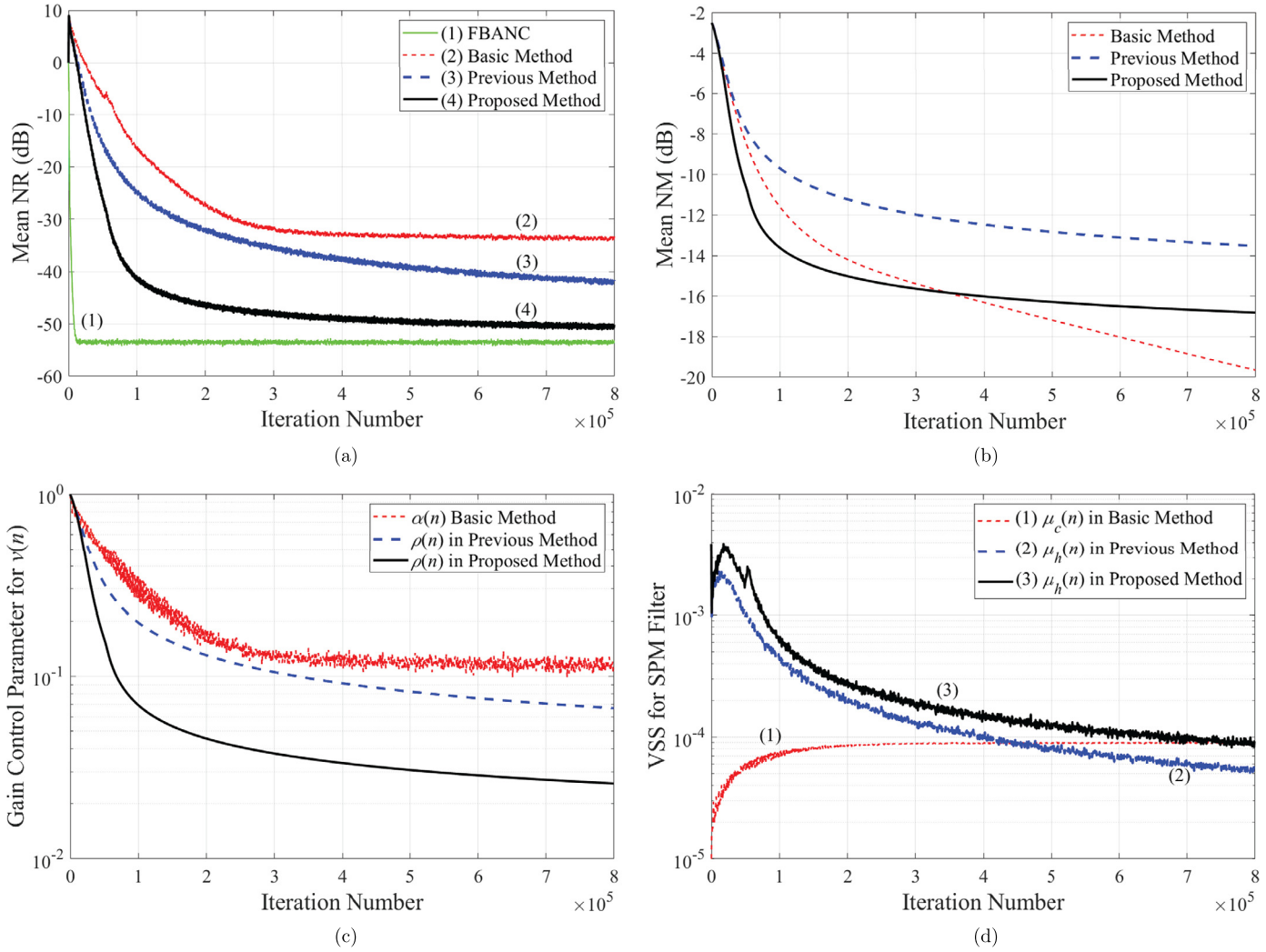

Fig. 10. Performance comparison between various methods for stationary acoustic paths. (a) Mean noise reduction (NR) (in dB), (b) Mean normalized misalignment (NM) (in dB), (c) Variation of the gain control parameter for probe signal $v(n)$, and (d) Variable step-size (VSS) for SPM filter.

the offline measurements are essential for implementation of practical ANC systems, therefore, assuming that SP filter is known a priori as $\hat{\boldsymbol{s}}(n) = \boldsymbol{s}(n)$, the conventional FBANC of Fig. 1 has been considered as a benchmark method as far as the NR performance is concerned.

2. The 'basic method' [27] which builds upon [14] for the FFANC systems. As stated earlier, the method in [28] is also based upon [14] and adds a few heuristically selected thresholds, and hence is not included in the performance comparison in this paper.
3. The previous method as presented in [29].
4. The proposed method which may be considered as a modified version of the previous method (see Section 3.1 for details).

In the results presented in this case study, the objective is to investigate the convergence speed and the steady-state NR performance for various methods for FBANC with online SPM. The simulation parameters for various methods for FBANC with online SPM are adjusted for fast and stable convergence of the respective method. The length of the SPM filter $\hat{\boldsymbol{s}}(n)$ is same as that of the true SP $\boldsymbol{s}(n)$, i.e., $M = 128$ in the basic method. In the previous and proposed methods, the appended delay z^{-D} is selected as $D = 8$ samples and hence the length of the composite SPM filter $\boldsymbol{h}(n)$ is $D + M = 136$. The step-size for ANC adaptive filter $\boldsymbol{w}(n)$ in the basic method (Fig. 2) is adjusted to $\mu_w = 1 \times 10^{-7}$. The basic method employs the modeling signal $v(n)$ being computed using (9) where $v_0(n)$ is zero-mean white Gaussian noise of variance 0.75. The step-size parameters for the adaptive SPM filter are selected as $\mu_1 = 1 \times 10^{-5}$ and $\mu_2 = 1 \times 10^{-4}$, and the corresponding VSS $\mu_c(n)$ is computed using (8d). The empirical parameters in the lowpass estimators in (8a) and (8b) are selected as $\lambda = 0.9$ and $\gamma = 0.01$. The step-size for ANC adaptive filter $\boldsymbol{w}(n)$ in the previous and proposed methods (Fig. 3) is adjusted to $\mu_w = 5 \times 10^{-7}$. The values of various parameters in computing the normalized VSS $\mu_h(n)$ (in (16)) are selected as $\hat{\mu} = 5 \times 10^{-3}$ (fixed step-size in the previous method and a semi-fixed one in the proposed method), $\mu_{h_{\min}} = 1 \times 10^{-5}$ (the lower bound on the steps-size value), and $\epsilon = 0.25$ (the regularization parameter to avoid division by zero). In the algorithm for convergence monitoring and change detection, the threshold on the parameter $\rho(n)$ is selected as $T1 = 0.15$ and $T2$ is a dynamic one being updated as long as the ANC systems remains in convergence (see Table 2). The additive random signal is same as in the basic method. The simulation results for various performance measures and behavior of various parameters are summarized in Figs. 10–12.

The curves for mean NR (in dB) for various methods are plotted in Fig. 10(a). It is observed that the standard FBANC system gives the best NR performance, which is obvious as it has a luxury of a perfect estimate of the SP. This performance in fact can be used as a benchmark to assess the performance of the rest of methods

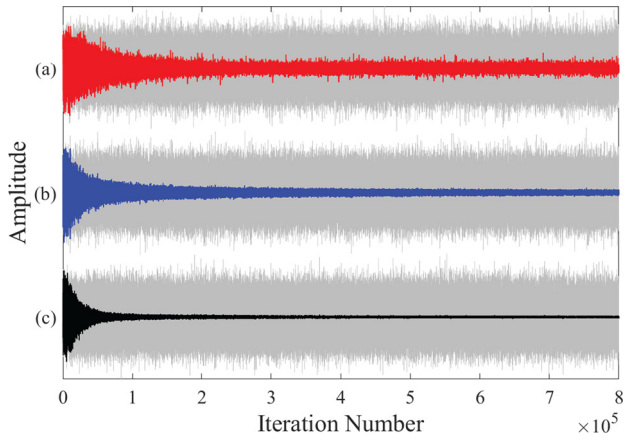

Fig. 11. Variation of probe signal $v(n)$ (color) in comparison with the additive random noise $v_0(n)$ (light-gray) for (a) the basic method, (b) the previous method, and (c) the proposed method.

equipped with online SPM. It is observed that the basic method falls far behind the rest, as far as the NR performance is concerned. The main reason lies in the way the additive random noise $v_0(n)$ is regulated to generate the modeling signal $v(n)$. The gain control parameter $\alpha(n)$ in the basic method is computed as ratio of the error signals' powers $P_{e_c}(n)$ and $P_e(n)$ (see (8c) and (9)).

It is worth to mention that the output $y(n)$ of the ANC adaptive filter is expected to take care of the disturbance signal $d(n)$ (see (6)), however, the component due to modeling signal remains there always at the error microphone (this is why we want to regulate the modeling signal at the first place). As seen in (7), the error signal $e_c(n)$ (and hence $P_{e_c}(n)$) will reduce (ideally converge to zero), if both the ANC adaptive filter $\boldsymbol{w}(n)$ and the SPM filter $\hat{\boldsymbol{s}}(n)$ converge. Since the same error signal $e_c(n)$ is used to adapt the two adaptive filters as well as to compute the parameter $\alpha(n)$, there is a strong intrusion between two adaptation process.

Consider the results presented in Fig. 10(c) for the adaptation of the gain control parameters. It is observed that the parameter $\alpha(n)$ does decay as the ANC system converges; however, settles to a somewhat larger value as that obtained for the gain control parameter $\rho(n)$ in the previous and proposed methods. Thus the modeling signal in the basic method settles to a large level and results in a poor NR performance. The VSS $\mu_c(n)$ in the basic method (computed using (8d)) increases the value of the step-size as $\alpha(n)$ decreases. This somewhat improves the convergence of the SPM filter $\hat{\boldsymbol{s}}(n)$ (see curves for mean NM (in dB) as shown in Fig. 10(b)); however, cannot improve upon the NR as $\alpha(n)$ does not become too small.

In the previous and proposed methods, the gain control parameter $\rho(n)$ (for the modeling signal) is computed using a delay-based processing which turns out to be a far superior strategy as compared with computing $\alpha(n)$ in the basic method. As stated earlier, the parameter $\rho(n)$ is computed using the initial coefficients of the composite SPM filter $\boldsymbol{h}(n)$, which would coverage to zeros (to model the appended delay). This is indeed observed in Fig. 10(c), with $\rho(n)$ converging to a smaller value in the proposed method as compared to that in the previous method (thanks to the modifications suggested in this paper). This reduces the modeling signal $v(n)$ to a very low level as observed in plots for $v(n)$ in comparison with the additive random noise $v_0(n)$ as shown in Fig. 11 for a typical realization. This has a substantial impact on the NR performance of the proposed method.

It is noticed from the results presented in Fig. 10(a) that the proposed method gives the best NR performance. As soon as ANC system converges, the modeling signal $v(n)$ becomes very low which in turn makes the convergence of the SPM filter very sluggish. This is indeed observed in the previous method (see mean NM curves in Fig. 10(b)). This is somewhat compensated in the proposed method as explained in Section 3.1. It is observed from the results shown in Fig. 10(d) that the normalized VSS $\mu_h(n)$ in the proposed method is (almost) always larger than that in the previous method. This results in the fast convergence of SPM filter in the proposed method as depicted by the curves for mean NM plotted in Fig. 10(b).

The steady-state spectrum for the residual error signal $e(n)$ for various methods is plotted in Fig. 12 for one realization. The plots for various methods are given in separate panels for a clarity of presentation, and spectrum of the primary disturbance $d(n)$ is included for comparison. The overall performance of the proposed method is better than that of the rest of methods, in reducing the tones present in the disturbance signal $d(n)$. It is important to consider the computational complexity comparison here. Using the expressions presented in Section 3.2, the basic method [27] would require 1037 multiplications, 1027 additions and 1 division per iteration for simulation conditions considered in this paper. The previous method [29] requires 1211 multiplications, 1049 additions and 3 division per iteration, and in addition the proposed method would require one more multiplication and one division per iteration. It is plausible that both previous and proposed method give much improved NR performance which is achieved at an expense of a slightly increased computational complexity as compared with the basic method. Last but not least, the proposed method clearly outperforms the rest of the methods considered in this paper.

4.4. Performance comparison for non-stationary acoustic environment

In the present case study, simulations have been carried out to investigate the performance in the situation of a sudden change in the acoustic environment. As stated earlier, such a situation may arise when there is a sudden and drastic movements in the area where ANC is deployed. Another possibility is sudden change of humidity, temperature, air flow, etc., in the area. In order to mimic such a scenario of sudden change, at the middle of simulation the coefficients of the $\boldsymbol{p}(n)$ are sign reversed and that of the SP $\boldsymbol{s}(n)$ are changed to a new values as shown in Fig. 7 for the gain reduction of 0.35. The reference signal and the other simulation parameters are same as in the previous case.

The simulation results for various performance measures are presented in Figs. 13 and 14. As observed in the previous case study on the influence of modeling error, the conventional FBANC system having a fixed (non-adaptive) SPM filter becomes unstable when the acoustic paths change during the middle of simulation. The reason is quite obvious that the modeling error between $\boldsymbol{s}(n)$ and $\hat{\boldsymbol{s}}(n)$ is too significant for the conventional FBANC system to stay stable.

It is observed that all methods equipped with online SPM perform very well as far as the robustness against the sudden change is concerned. The basis method gives an improved performance from the view point of SPM (especially after the change in acoustic paths) as shown in Fig. 13(b), however, does not exhibit good NR performance (see Fig. 13(a)). The reason lies in the fact that the gain control parameter $\alpha(n)$ (see Fig. 13(c)) settles to a large value, and hence a large modeling signal $v(n)$ (see curve (a) in Fig. 14) is present in the ANC system. This large level modeling signal gives fast convergence for the modeling filter, however, severely degrades the NR performance.

The main task of any ANC system is to provide NR around the error microphone location and the proposed method does this job very well as in the previous case. In fact, the proposed method gives the best NR performance before as well as after the sudden change. Furthermore, it improves upon the modeling accuracy of

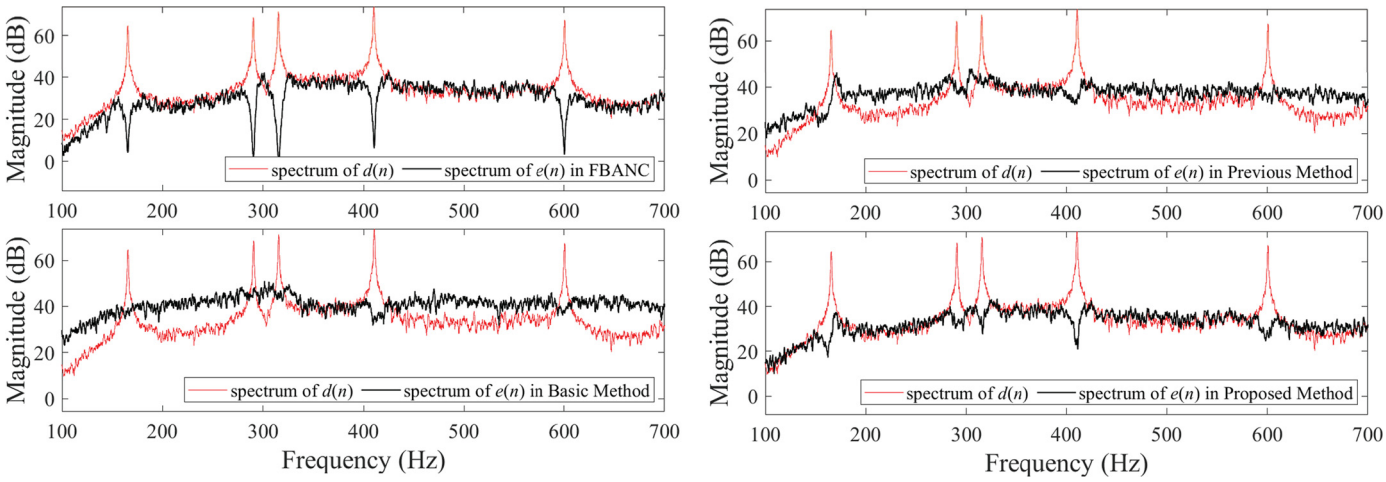

Fig. 12. Spectrum of the residual error signal $e(n)$ at the steady-state in comparison with that of the primary disturbance $d(n)$. (top-left) FBANC with fixed SPM filter, (bottom-left) the basic method, (top-right) the previous method, and (bottom-right) the proposed method.

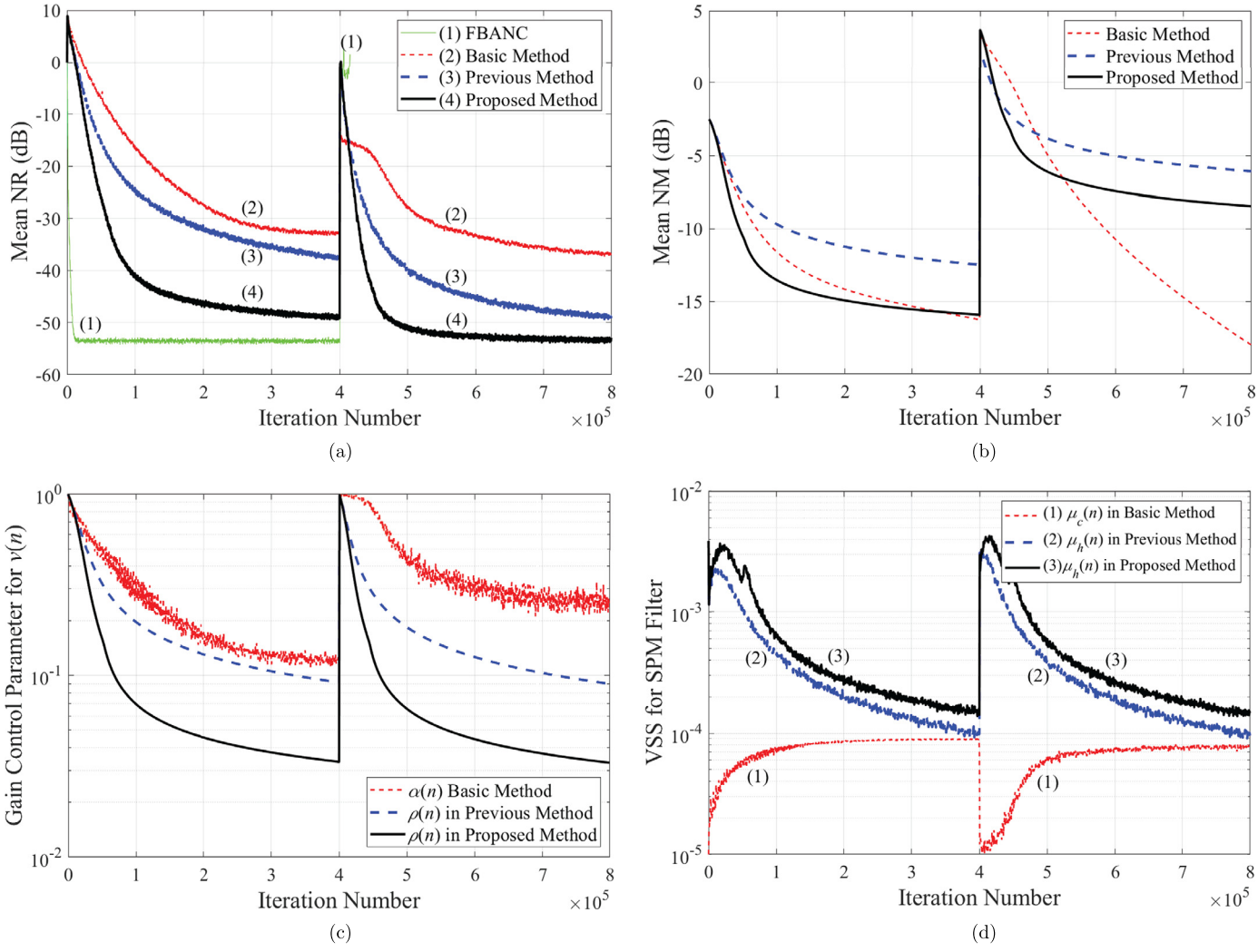

Fig. 13. Performance comparison between various methods for non-stationary acoustic paths having a sudden change during the middle of simulation. (a) Mean noise reduction (NR) (in dB), (b) Mean normalized misalignment (NM) (in dB), (c) Variation of the gain control parameter for probe signal $v(n)$, and (d) Variable step-size (VSS) for SPM filter.

SPM filter as compared with the previous method. This improved performance in the proposed method can be explained by observing the various results as follows. The gain control parameter $\rho(n)$ (Fig. 13(c)) becomes very small at the steady-state, resulting is reducing the modeling signal (curve (c) in Fig. 14) and hence giving the best NR performance (Fig. 13(a)). In addition to this, the normalized VSS parameter $\mu_h(n)$ (Fig. 13(d)) stays large as compared with that in the previous method. This improves the modeling ac-

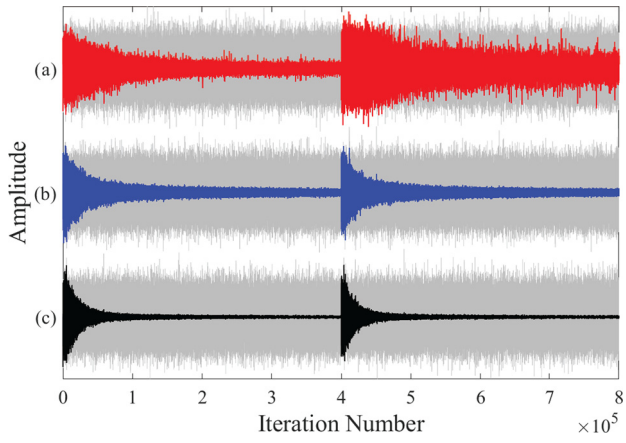

Fig. 14. Variation of probe signal $v(n)$ (color) in comparison with the additive random noise $v_0(n)$ (light-gray) for (a) basic method, (b) the previous method, and (c) the proposed method, for simulations with non-stationary acoustic paths having a sudden change during the middle of simulations.

curacy of the SPM filter, which further aids in the NR performance of the overall ANC system.

5. Conclusions

This paper develops an efficient method for the FBANC systems when simultaneous adaptation of ANC and SPM filters is needed. The proposed method injects an uncorrelated random noise as a modeling signal for the adaption of the SPM filter. By employing a delay-based adaptation [31,32] for the SPM filter, a time-varying gain parameter is tuned online to control the level of the modeling signal. The idea is to track the convergence status of the SPM filter, such that the level of modeling signal is reduced as soon as the system converges. This has plausible impact on the NR performance of ANC system, as demonstrated by detailed simulation results presented earlier. The presented numerical results show that the proposed method gives the best NR performance, in fact very close to that achieved by the conventional FBANC system having an exact estimate of the SPM filter $\boldsymbol{s}(n)$. It is important to mention that the proposed method gives an improved NR performance, and yet with adding just a negligible computational complexity to the previous method presented in [29].

One limitation of the proposed method is its ability to work with only the narrowband noise sources. This is in fact is due to the basic structure of the FBANC system which requires noise source to be predictable. In many practical scenarios the target noise may be comprised of a mix of both narrowband as well as broadband components. In such cases, it is recommended to employ a hybrid ANC structure which comprises feedforward as well as feedback parts [33]. It would be interesting to extend the proposed method for such hybrid ANC systems. Furthermore, it will be interesting to explore in future if the injection of the additive random noise can be completely stopped at the steady-state.

CRediT authorship contribution statement

Muhammad Tahir Akhtar: Conceptualization, Funding acquisition, Investigation, Methodology, Project administration, Software, Validation, Visualization, Writing – original draft, Writing – review & editing.

Declaration of competing interest

The authors declare that they have no known competing financial interests or personal relationships that could have appeared to influence the work reported in this paper.

Acknowledgments

A part of this work was carried out whilst Dr. Akhtar was a short-term visiting researcher at the COPPE Federal University of Rio de Janeiro, Brazil and supported by the Social Policy Grant (SPG) of Nazarbayev University. Furthermore, this research has been partially funded from the Faculty Development Competitive Research Grants Program of Nazarbayev University under the Grant Number 110119FD4525. Finally, thanks are due to the anonymous reviewers for providing many critical and insightful comments. This has helped in substantially improving the contents, organization, and quality of presentation of the manuscript.

References

[1] WHO Regional Office for Europe, Environmental Noise Guidelines for the European Region (2018): WHO Regional Office for Europe, WHO Regional Office for Europe, ISBN 978-92-890-5356-3, 2018. Available online, https://www.euro.who.int/en/publications/abstracts/environmental-noise-guidelines-for-the-european-region-2018.
[2] M.T. Akhtar, An adaptive algorithm - based on modified tanh non-linearity and fractional processing - for impulsive active noise control systems, J. Low Freq. Noise Vib. Act. Control 37 (3) (Sept. 2018) 495–508.
[3] P. Lueg, Process of silencing sound oscillations, US Patent, 2043416, June 9, 1936.
[4] S.M. Kuo, D.R. Morgan, Active Noise Control Systems-Algorithms and DSP Implementations, Wiley, New York, 1996.
[5] S.M. Kuo, D.R. Morgan, Active noise control: a tutorial review, Proc. IEEE 87 (1999) 943–973.
[6] Y. Kajikawa, W.S. Gan, S.M. Kuo, Recent advances on active noise control: open issues and innovative applications, APSIPA IEEE Trans. Signal Inf. Process. 1 (Dec. 2012) e3.
[7] P.N. Samarasinghe, W. Zhang, T.D. Abhayapala, Recent advances in active noise control inside automobile cabins, IEEE Signal Process. Mag. 33 (6) (Nov. 2016) 61–73.
[8] B. Lam, W.S. Gan, Active acoustic windows: toward a quieter home, IEEE Potentials 35 (1) (Jan.-Feb. 2016) 11–18.
[9] C.Y. Chang, A. Siswanto, C.Y. Ho, T.K. Yeh, Y.R. Chen, S.M. Kuo, Listening in a noisy environment, IEEE Consum. Electron. Mag. (Oct. 2016) 34–43.
[10] B. Farhang-Boroujeny, Adaptive Filters: Theory and Applications, 2nd edition, John Wiley & Sons, 2013.
[11] D.R. Morgan, An analysis of multiple correlation cancellation loops with a filter in auxiliary path, IEEE Trans. Acoust. Speech Signal Process. ASSP-28 (Aug. 1980) 454–467.
[12] S.J. Elliott, I.M. Stothers, P.A. Nelson, A multiple error LMS algorithm and its application to the active control of sound and vibration, IEEE Trans. Acoust. Speech Signal Process. ASSP-35 (Oct. 1987) 1423–1434.
[13] N. Saito, T. Sone, Influence of modeling error on noise reduction performance of active noise control systems using filtered-x LMS algorithm, J. Accoust. Soc. Jpn. (E) 17 (4) (Apr. 1996) 195–202.
[14] M.T. Akhtar, M. Abe, M. Kawamata, A new variable step size LMS algorithm-based method for improved online secondary path modeling in active noise control systems, IEEE Trans. Audio Speech Lang. Process. 14 (2) (Mar. 2006) 720–726.
[15] S. Ahmed, M.T. Akhtar, X. Zhang, Robust auxiliary-noise-power scheduling in active noise control systems with online secondary path modeling, IEEE Trans. Audio Speech Lang. Process. 21 (4) (Apr. 2013) 749–761.
[16] P.A.C. Lopes, J.A.B. Gerald, Auxiliary noise power scheduling algorithm for active noise control with online secondary path modeling and sudden changes, IEEE Signal Process. Lett. 22 (10) (Oct. 2015) 1590–1594.
[17] Y.J. Chu, A new regularized subband ANC algorithm with online secondary-path modeling: performance analysis and application to buildings, Build. Environ. 94 (Part 2) (Dec. 2015) 873–882.
[18] C.Y. Chang, S.M. Kuo, C.W. Huang, Secondary path modeling for narrowband active noise control systems, Appl. Acoust. 131 (Feb. 2018) 154–164.
[19] M. Tufail, S. Ahmed, M. Rehan, M.T. Akhtar, A two adaptive filters-based method for reducing effects of acoustic feedback in single-channel feedforward ANC systems, Digit. Signal Process. 90 (Jul. 2019) 18–27.
[20] S. Ahmed, M.T. Akhtar, Gain scheduling of auxiliary noise and matching step-size for online acoustic feedback cancelation in narrow-band active noise control systems, IEEE/ACM Trans. Audio Speech Lang. Process. 25 (2) (Feb. 2017) 333–343.
[21] H.S. Vu, K.H. Chen, A high-performance feedback FxLMS active noise cancellation VLSI circuit design for in-ear headphones, Circuits Syst. Signal Process. 36 (7) (Jul. 2017) 2767–2785.
[22] L. Wu, X. Qiu, Y. Guo, A generalized leaky FxLMS algorithm for tuning the waterbed effect of feedback active noise control systems, Mech. Syst. Signal Process. 106 (Jun. 2018) 13–23.

[23] P.R. Benois, U. Zölzer, Psychoacoustic optimization of a feedback controller for active noise cancelling headphones, in: Proc. 26th International Congress Sound Vibr, Montreal, Canada, Jul. 2019.
[24] P.R. Benois, P. Nowak, E. Gerat, M. Salman, U. Zölzer, Improving the performance of an active noise cancelling headphones prototype, in: Proc. Inter-Noise 2019, Madrid, Spain, Jun. 2019.
[25] S. Liebich, J. Fabry, P. Jax, P. Vary, Acoustic path database for ANC in-ear headphone development, in: Proc. 23rd Inter. Cong. Acoustics (ICA), Sep. 2019, pp. 4326–4333.
[26] J. Fabry, P. Jax, Primary path estimator based on individual secondary path for ANC headphones, in: Proc. IEEE ICASSP 2020, May 2020, pp. 456–460.
[27] M.T. Akhtar, A fully adaptive feedback ANC system employing online estimation of the cancellation path, in: Proc. IEEE MWSCAS 2019, Aug. 04-07, 2019, Dallas, TX, USA, 2019, pp. 674–677.
[28] H. Hassanpour, P. Davari, An efficient online secondary path estimation for feedback active noise control systems, Digit. Signal Process. 19 (2) (Mar. 2009) 241–249.
[29] M.T. Akhtar, Adaptive feedback active noise control (AFB-ANC) system equipped with online adaptation and convergence monitoring of the cancellation-path estimation (CPE) filter, in: Proc. IEEE GlobalSIP 2019, Nov. 11-14, 2019, Ottawa, Ontario, Canada, 2019.
[30] M.T. Akhtar, On adaptation of cancelation path modeling filter in single-channel feedback-type adaptive active noise control systems, in: Proc. IEEE MWSCAS 2020, Aug. 09-12, 2020, Springfield, MA, USA, 2020, pp. 852–855.
[31] A. Mader, H. Puder, G.U. Schmidt, Step-size control for acoustic echo cancellation filters–an overview, Signal Process. 4 (2000) 1697–1719.
[32] M.T. Akhtar, F. Albu, A. Nishihara, Acoustic feedback cancellation in hearing aids using dual adaptive filtering and gain-controlled probe signal, Biomed. Signal Process. Control 52 (Jul. 2019) 1–13.
[33] M.T. Akhtar, W. Mitsuhashi, Improving performance of hybrid active noise control systems for uncorrelated narrowband disturbances, IEEE Trans. Audio Speech Lang. Process. 19 (7) (Sept. 2011) 2058–2066.

Muhammad Tahir Akhtar received his PhD degree in Electronic Engineering from the Tohoku University, Sendai, Japan, in 2004, MSc in Systems Engineering from the Quaid-i-Azam University, Islamabad, Pakistan in 1999, and BSc Electrical (Electronics and Communication) Engineering from the University of Engineering & Technology, Taxila, Pakistan in 1997.

He is currently working as an Associate Professor at the School of Engineering and Digital Sciences, Nazarbayev University, Nur-Sultan City, Kazakhstan. From 2014 to 2017, he was an Associate Professor at the COMSATS University Islamabad, Pakistan. From 2008 to 2014, he was an Assistant Professor at the University of Electro-Communications, Tokyo, Japan, and a Special Visiting Researcher at the Tokyo Institute of Technology, Tokyo, Japan. He was a visiting researcher at Institute of Sound and Vibration Research (ISVR), University of Southampton, UK (Dec. 2008 - Feb. 2009), and at Institute for Neural Computations (INC), University of California San Diego (Nov. 2010 - Mar. 2011). Prior to that, he was a COE postdoctoral fellow at Tohoku University, Sendai Japan (2004-2005), and has worked as an Assistant Professor at the United Arab Emirates University, UAE (2006-2008).

His research interests include adaptive signal processing, active noise control, blind source separation, and biomedical signal processing. Dr. Akhtar has published about 95 papers in the peer-reviewed international journals and conference proceedings**.** He won Best Student Paper at the IEEE 2004 Midwest Symposium on Circuits and Systems, Hiroshima, Japan, and student paper award (with Marko Kanadi) at 2010 RISP International Workshop on Nonlinear Circuits, Communications and Signal Processing. He has been on the editorial board of Hindawi Advances in Mechanical Engineering (2013-2019), and a member of The European Association for Signal Processing (EURASIP) (2009-2011). He has been a member of Asia-Pacific Signal & Information Processing Association (APSIPA) (2010-2013), and has served as a co-editor for APSIPA newsletter (2011-2013). Currently he is member IEEE Signal Processing Society, IEEE Industrial Electronic Society, and he is a Senior Member IEEE.